HF RFID Reader for Mouse Identification - Study of Magnetic Coupling between Multi-Antennas and a Ferrite Transponder

C. Ripoll[1], P. Poulichet[1], E. Colin[2], C. Maréchal[2] and A. Moretto[2]

[1] Université de Paris-Est, Esiee, Esycom
Cité Descartes, BP99, 93162 Noisy le Grand Cedex
[2] Esigetel- Département de Télécommunications
1 rue du port de Valvins 77215 Avon-Fontainebleau

Abstract. This paper depicts an optimized RFID system operating at 13.56 MHz, used to recognize a mouse. When it passes near an antenna, the small transponder (1x6 mm^2) placed in its body communicates with the antenna. The distance of communication is small (around 3 centimeters) and our objective was to increase this distance. The transponder receives the signal from a coil wound around a magnetic circuit. The characteristics of the ferrite are very important for the communication. All the elements of the chain are taken into account in ADS simulation and we determine the value of the minimum voltage necessary for remote bias. Finite-element analysis is employed to extract the values of the generated magnetic field. The paper shows how to correlate the influent parameters to increase the communication distance. To improve this reading rate, a novel differential receiving antenna has been designed allowing an improved decoupling with the close transmitting antenna. An electrical model of the different parts has been performed. This includes the tag, the reader antennas and the coupling between them. These models have been validated by measurements and used for the simulations of the complete system.

1 Introduction

The principle used to identify a mouse is depicted on the figure 1. The biocompatible transponder of 1 mm in diameter and 6 mm in length is introduced under the skin of the mouse with a syringe. When the mouse passes in the vicinity of the transmitting Antenna, the transponder receives the signal from the antenna. The amplitude of the signal at 13.56 MHz has to be sufficient to supply the transponder and to transmit coded signal. It reacts by sending a coded signal in order to identify the mouse.

The inductive coupling RFID (Radio Frequency Identification) systems operating at 13.56 MHz are present nowadays in a large variety of applications, like access control, mass transport, e-purse and secured ID cards. In a conventional system, they are basically composed of one or more transponders dialoging with a base station by means of a coupling through the close-field magnetic induction. The base station produces a magnetic field that supplies power to the transponder, interrogates the tag

Ripoll C., Poulichet P., Colin E., Maréchal C. and Moretto A. (2008).
HF RFID Reader for Mouse Identification - Study of Magnetic Coupling between Multi-Antennas and a Ferrite Transponder.
In *Proceedings of the 2nd International Workshop on RFID Technology - Concepts, Applications, Challenges*, pages 32-42
DOI: 10.5220/0001728900320042

and decodes the information received.

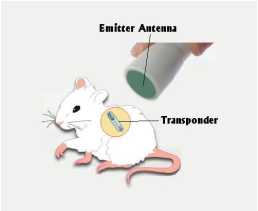

Fig. 1. Communication between the mouse and the Emitter antenna.

The two parts communicate in half-duplex mode: during the uplink, the base station sends a request (ASK-modulated, 100% or 10% modulation index, depending on radio interface type [1]) then it continues to transmit an unmodulated 13.56 MHz carrier, which supplies power to the transponder IC; during the downlink, the transponder responds by varying its load impedance, and thus modulating the carrier sent by the base station (847.5 kHz OOK or BPSK-modulated subcarrier, depending on radio interface type [1], switches between the impedance states), mechanism called load modulation. The carrier will thus be modulated in amplitude (AM) and phase (PM).

Current state-of-the-art in RF characterization of 13.56 MHz inductive coupling identification systems only involves a basic check of the standard compliance [1], [2]. Although reference transponder circuits are used, no electrical parameter measurement is performed.

In biomedical domain, where inductive links are used to deliver power and exchange information with implanted stimulators, results have been published [3] – [5], regarding the remote power supply in an inductive coupling system and its variation when the coupling changes. Concerning the measurement methods, a detailed analysis of coupled resonators is performed by Kajfez in [6], [7]. Majority of proximity coupling applications concern the magnetic resonance imaging and a very few for the RFID applications.

The RFID system can be modeled as a double-tuned transformer, whose primary represents the base station and secondary the transponder. The transponder, often called tag, is made out of an IC (integrated circuit) which capacitive input impedance resonates with an antenna coil that collects the magnetic flux.

Proximity Radio Frequency Identification (RFID) systems physically relies on the space evolution of their loop antennas mutual coupling, i.e. their shape, dimensions and relative position. In order to optimize the antennas design, one needs to predict the coupling evolution within the desired operating zone. Previous works in biomedical domain focused on the coupling variation, mainly for circular loops.

2 System Description and Design Keypoints

A well-designed RFID system should ensure a safe functioning within a precise geometric volume (i.e. voltage supply to the transponder IC and modulation depth compliant with the manufacturer's specifications).

Three entities can be distinguished, whose interdependence should be understood: the base station (i.e. antenna topology and detection threshold), the RF channel (i.e. magnetic radiation pattern) and the transponder (i.e. IC and antenna).
When the transponder moves in the field of the base station, the induced voltage at the IC input varies over a large range [4] (e.g. the magnetic field, varying between 1.5 and 7.5 A/m for systems compliant with [1], may induce a voltage of 5 to 35 V at the IC). Moreover, the logic part of the IC needs a regulated voltage supply and a current source, to avoid parasitic load modulation during its functioning. In these conditions, a voltage-and-current regulation system varies the input capacitance and load resistance of the IC. Thus, the overall functioning passes through a wide range of states, given that the load mismatch represented by the transponder on the base station antenna varies.
The aim of an RFID system used in biological experiments for identifying laboratory mice or small animals is to be able to read the ID code in the largest volume zone with the smallest transponder as possible to avoid stress and so unpredictable behavior of the animal. For this reason, the transponder used here is an ultra small transponder measuring only 1 by 6 mm encapsulated in a glass capsule. The system operates in the world-wide ISM band of 13.56 MHz and not the classical 134 kHz band used for animals, so as to reduce the size of the transponder antenna. With such a tiny small transponder, it becomes compulsory to use a coil antenna wounded on a ferrite rod to increase the induced voltage.
Before introducing the key points of this study, let us recall that the system operates with the same minimal constraints as in any conventional proximity passive RFID system. This means that we should take into account the remote biasing of the transponder but as well the data exchange between the reader and the tag in a Listen Before Talk protocol. In our case, to remote bias the transponder, first we must radiate a high magnetic field, which means that a high current circulates through the transmitting coil and second, the Q factor of the transponder should be optimized to be rather high but not too high to avoid degrading the backscatter modulation bands placed at +/- 848 kHz. These constraints call for a precise modeling of the transponder parameters and particularly the Q factor. We note that in contrary to a smart card reading system, we can here neglect the variations of the transfer function (i.e. band-pass shape, resonance and Q-factor) as the coupling varies [3], [6].
Unfortunately, modeling such a tiny rod is theoretically unreliable due to the difficulty to measure the magnetic losses, which are expressed by the μ_r'' of the material. Consequently, the modeling will be based on the measurements of a resonant transponder.
Another key point in this study was to avoid the coupling between transmitter and receiver. In the transmitter path, very high voltage exists due to the matching circuits and to the high current as we already mentioned. To reduce dramatically this problem, we used a differential antenna on the receiver side. This design allows the perfect cancellation of the carrier transmitted by the transmitting antenna when the coils are ideally balanced. As a drawback for this geometrical configuration, we should mention that the data exchange becomes impossible for a central position of the mouse. This is of little importance because the mouse ID code has the opportunity to be read at many points when it enters the bean-shaped reading zone. Obviously, the coupling is finite and the topology of the receiver should take this into account.

This work is organized as follows. Section 3 presents the magnetic simulations of the transmitting antenna. It shows the influence of the permeability of the transponder. Section 4 describes the electrical modeling of the three parts (transponder, transmitter and receiver). In Section 5, we perform electrical simulations of the complete system.

3 Magnetic Simulations of the Antennas

The figure 2 shows the shape of the transmitting antenna. It is realized with a round PCB of diameter of 3 cm. The outside circular trace of each side of the PCB is used to generate the transmitting magnetic field. The two inner spirals that constitute the differential antenna used for the reception are connected together and one point is connected to the ground.

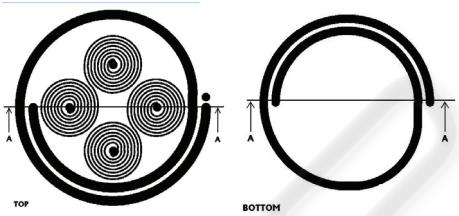

Fig. 2. Shape of the transmitting antenna and differential antenna.

The simulation is operating using 2 dimensions FEM (Finite Element Modeling) with Ansys [8]. Figure 3 represents the model used for FEM. It represent a cut along the axis A-A of the figure 2. The permeability μ_r' (120 for ferrite of the transponder), the resistivity σ of the materials and the current in the conductors are taken into account in order to determine the magnetic field in magneto dynamic simulations.

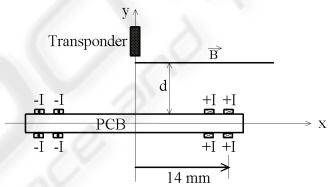

Fig. 3. Geometry for the FEM.

A measurement of the inductance of the transmitting antenna shows that the spiral inductance has no effect on the magnetic field so they are not taken into account in the simulation.

Figure 4 shows the module of the magnetic induction (B) determined in axis-symmetric simulation. The high permeability of the transponder concentrates the magnetic field generated by the current in the transmitting antenna. This permeability is a key point design because a high value increases the distance of reception. However, it is difficult to obtain a high value at 13.6 MHz without loss.

We determine the magnetic induction (B) at distances d of 0.5 cm, 1 cm, 2cm and 3 cm. The curve is represented on the figure 5.

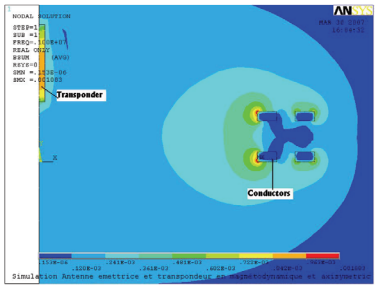

Fig. 4. B values near the transmitting antenna.

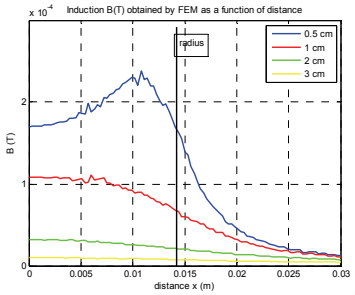

Fig. 5. Magnetic induction B (T) with respect to distance d on a parallel line for x=0.

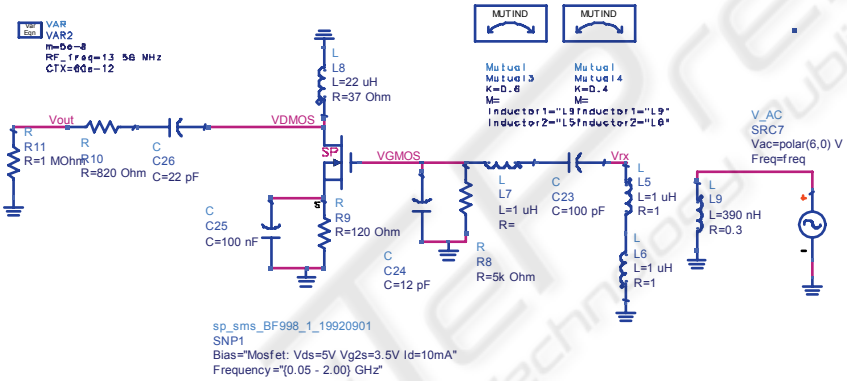

Fig. 6. Differential receiver schematic.

When the distance d increases, the magnetic induction B is reduced. When the distance x is higher than the radius of the transmitting antenna, the induction B is reduced.

4 Characterization Receiver, Transmitter and Transponder

To be able to optimize the whole system, we have to study the individual components.

4.1 Measurements of the Parameters of the Receiver

The electrical circuit of the receiver is shown in figure 6. Its transfer function is simulated by injecting a signal through a non resonant generator inductively coupled (L9 transmitting antenna) to the two coils representing the differential spiral antennas in figure 2 and L5-L6 in figure 6. The received signal is transmitted through a band-

pass (C23-L7-C24) to the MOS transistor used to amplify the signal. The circuit is designed so that its transfer function is centered on 14.4 MHz frequency that corresponds to one of the symmetric backscattered bands around the 13.56 MHz carrier. We have to mention that the parallel resistance R8 allows the setting of the bandwidth, so is influent for the filtering of the carrier residual and will have an impact on the distortion of the modulated bandwidth.

4.2 Measurements of the Parameters of the Transmitter

The schematic of the transmitter is represented in figure 5. M2 is a MOS transistor operating in a low loss switching mode. It generates a high current circulating in the transmitting antenna L1. C13, C22//C21//C12 and L1 constitute a parallel resonant circuit. C21 or Ctx is a variable capacitor adjusted to facilitate the remote bias of the transponder. Frequency analysis has to be taken into account as a first step to adjust the resonant frequency. Furthermore, the shape of the voltage across the transmitting antenna has to respect a standard waveform (see 4.2.2).

4.2.1 Frequency Analysis

The transfer function is simulated with a sinusoidal excitation, then we derive for which value of Ctx, we obtain a maximized current (I_Probe) in the transmitting coil. The resonant frequency has to be set up at 13.56 MHz to induce the necessary voltage at the input of the IC tag. This is achieved through the use of the Ctx parallel capacitor.

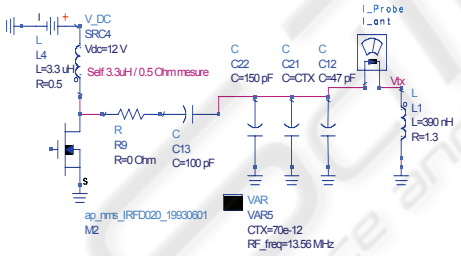

Fig. 7. Transmitter schematic.

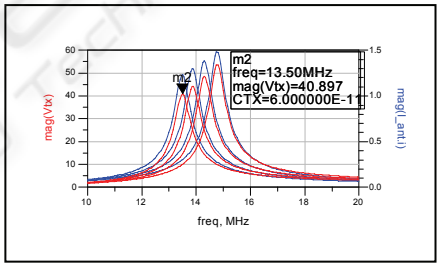

Fig. 8. Variation of the Transmitter transfer function with variable Ctx values.

As shown in figure 8, the transfer function is a band-pass type which quality coefficient has to be around 30 to avoid degradation of the 200 kHz modulation bandwidth around the carrier.
Figure 8 represents the shift of the central frequency as a function of Ctx. We note that it is preferable for the transmitter not to operate at 13.56 MHz (Ctx=70pF) but rather near this frequency. For example, we obtained best results for a value of 14.4 MHz (Ctx=35pF).

4.2.2 Temporal Analysis

We should consider the time domain response because, to operate properly, any Mifare UltraLight IC at the tag should be able to detect the presence of a pause in the transmitted signal. This means that the matching / filter circuit should respect the waveform shown in figure 9.

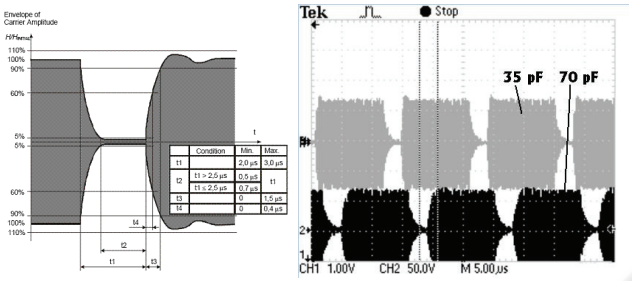

Fig. 9. Standard waveform and Measured voltages at and near resonance (Ctx=35pF and 70 pF).

The table 1 shows that times t2 and t4 depend largely of the value of Ctx. In the case of 35 pF, t2 is near of the minimal value and with 70 pF, t2 is too low. For Ctx = 70 pF, the distance of detection of the transponder is likely to be too small.

Table 1. Comparison between ISO14443 and simulated results for transmitter operating at and near resonance.

t1=2 uS	Min	Max	Ctx=35 pF (near)	Ctx=70 pF (at resonance)
t2 (5% decay time)	0.7 uS	t1	0.6 us	0.5 us
t3 (90% rise time)	0	1.5 uS	0.33 uS	1.22 uS
t4 (60% rise time)	0	0.4 uS	0.19 uS	0.51 uS

4.3 Measurements of the Parameters of the Transponder

Because the parameters have to be extracted in a non destructive test, we use a contactless methodology. The transponder was placed in a test primary coil shown in figure 10. The resistance Re and inductance Le of this coil have been characterized with an impedance analyser. Then the mutual coefficient between this primary coil and a transponder without its IC has been extracted by measurement of the induced voltage at the open transponder coil.

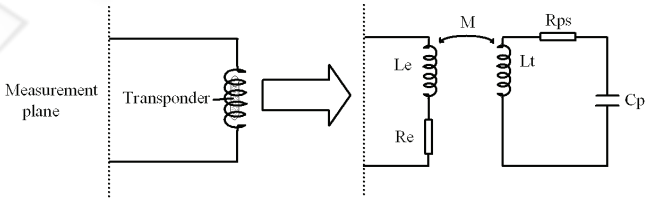

Fig. 10. Set-up to measure the parameters of the transponder.

The equation giving the impedance at the primary coil is:

$$Zp = jL_e\omega + R_e + \frac{M^2\omega^2}{jL_t\omega + R_t + R_{ps} + 1/\ jC_p\omega} \quad (1)$$

Rt, Lt: Series resistance and inductance of the transponder coil without ferrite.
Lt: Inductance of the transponder coil with ferrite.
Rps: Series resistance due to magnetic losses.
Cp: input capacitance of the IC.

By measuring the resonance frequency, input resistance and reactance at the primary coil, one can extract the frequency at which denominator cancels. So, because the input capacitance is known, the value of secondary inductance and resistance are extracted.

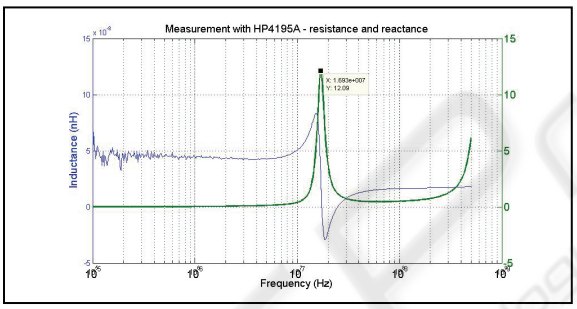

Fig. 11. Measurement of input impedance at primary coil.

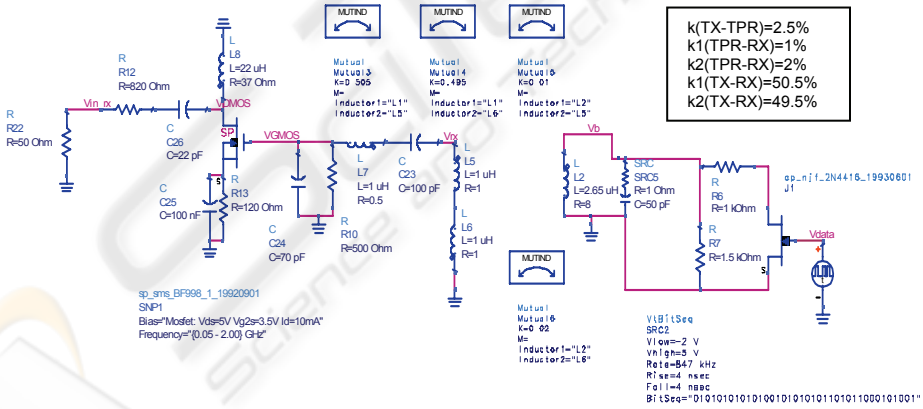

Fig. 12. Complete system (Transmitter not represented but all mutual inductances are present).

5 Characterization of the Complete System

Now we can proceed to the simulation of the complete system. All the individual elements have been optimized according to known criteria as for example to

maximize the radiated H field or to center the RX filter onto one backscattered side band. The position of the mouse when crossing the reading volume is taken into account by considering variable coupling coefficients between the transponder TPR and receiver RX. As shown in figure 5, the magnetic induction received by the transponder changes and the coupling coefficient follows.
In figure 12, the complete system is represented (note that transmitter does not appear for clarity) with all the mutual coefficients between transmitter TX, receiver RX and transponder TPR.
The coupling coefficients k (TX-RX) between TX and RX are made variable. The tests are performed for weak coupling (transponder in the farthest zone) and for a non ideal coupling (zero coupling) between transmitter antenna and differential receiver antennas:
The differential antenna system has been modelized by two coils in series which induced currents are inverted according to the reference dot (simulates the inverted windings of the spirals). In the case of ideal coupling between Tx and Rx, the induced voltages in the spiral antennas is null. To account for the non ideal case, we consider non equal mutual coefficients.
We note important results in table 2. Even in the case where there is no coupling between the transponder and the receiver (f1), a modulated signal is present as shown in figure 14. Actually, it comes from the transmitter which is coupled to the transponder. So, it means that even in the case of null coupling, because the transmitter and the receiver antennas cannot be perfectly uncoupled, data exist in the receiver.

Table 2. Received modulated voltage with different TPR to RX coupling coefficients.

Vrx	No coupling to TPR-RX	With equal coupling k1=0.01 k2=0.01	With unequal coupling k1=0.01 k2=0.02	With no Tx-Rx coupling k1=0.02 k2=0.01
	60mV f1	60mV f2	62mV f3	140mV f4

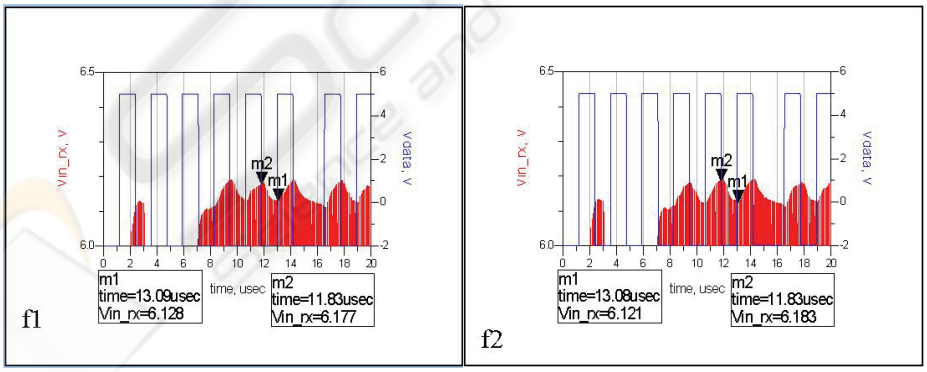

Fig. 13. Waveforms at the receiver for 4 case studies:
f1: with no coupling between Tpr-Rx and coupling between Tx-Rx.
f2: with equal coupling between Tpr-Rx and coupling between Tx-Rx.

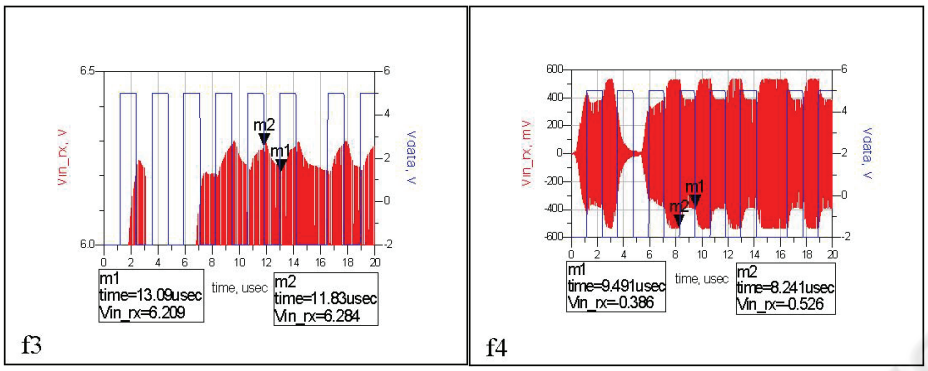

Fig. 14. Waveforms at the receiver for 4 case studies (cont.):
f3: with unequal coupling between Tpr-Rx and coupling between Tx-Rx.
f4: with unequal coupling between Tpr-Rx and no coupling between Tx-Rx.

We can even add that this is the main coupling mechanism because in the case of coupling between transponder and receiver (f2, f3), the modulation voltages are of the same order. Besides, this extra coupling has the effect of multipath summation in propagation. It means that we can distort the shape of the received data. This is confirmed by the last case (f4) in figure 14 where we nullified the coupling between transmitting and receiving antennas (ideal operation mode). We observe that amplitude is more than double and much closer to the generated square waveform from the transponder.

6 Conclusions

To optimize an RFID reader magnetically coupled to a tiny ferrite transponder, compromises have to be made. On the transmitter side, the matching circuit between the switching MOS transistor and the coil antenna is optimum and should be tuned at 13.56 MHz to maximize the radiated H-field so as to maximize the transponder induced voltage. This matching circuit should be tuned slightly above 13.56 MHz if waveform of the modulated signal (pause) is to be fit with the ISO14443 recommendation. On the receiver side, the matching circuit between the differential coil antennas and the Low Noise Amplifier is to be centered on the side band (13.56 MHz plus the subcarrier frequency = 14.4 MHz) with a bandwidth that should preserve the integrity of the modulation data. As for the transponder, it is a key element and the ferrite itself should be chosen with great care due to the detrimental effect of too high magnetic losses. In the extracted model, we found 8 Ohms for the equivalent resistance which is the primary factor to determine the Q, here 10. This quality factor means a bandwidth of around 1.5 MHz, which is necessary to preserve a sufficient bandwidth to receive and send the data from and to the transmitter. Due to the shape of the rod, the effective permeability is much less than the relative permeability. We computed and measured an effective μ_r' of 14 for a relative μ_r'of 120. To determine the induced voltage, magnetic simulations have been performed so as to calculate the B field at any point in the reading volume.

A differential receiving antenna to avoid the strong voltage which occurs in classical HF systems has been designed. We managed to obtain a reduced coupling with safe voltage values. We noticed as well that this imperfect coupling means an intermediate path for the data to couple from the transponder to the receiver. In consequence, the reading volume is larger than foreseen, because there is no dead zone but as a drawback, the data may be distorted. To reduce the Tx-Rx coupling, the Tx antenna is built with two coils, one on each side of the board to insure the symmetry with the spiral antennas.
In conclusion, an HF reader has been simulated, built and optimized to reach a reading distance of about 3 cm for an ultra-small ferrite transponder injected under the skin of the mouse.

References

1. "Identification cards - Contact less integrated circuit(s) cards - proximity cards", ISO / IEC 14443 – 2 international standards, Part 2 "Radio frequency power and signal interface".
2. "Identification cards – test methods", ISO / IEC 10373-6 international standard, Part 6 "proximity cards".
3. N. Chaimanonart, K. R. Olszens, M.D. Zimmerman, W.H. Ko, D.J. Young, “Implantable RF Power Converter for Small Animal In Vivo Biological Monitoring” Engineering in Medicine and Biology Society, 2005. IEEE-EMBS 2005. 27th Annual International Conference, 2005 pp 5194 – 5197.
4. M. Soma, D. C. Galbraith, R. L. White, "Radio-frequency coils in implantable devices: misalignment analysis and design procedure", IEEE Trans. on biomedical engineering, vol. BME-34, No. 4, pp 276-282, April 1987.
5. C. M. Zierhofer, E. S. Hochmair, "Geometric approach for coupling enhancement of magnetically coupled coils", IEEE Trans. on biomedical engineering, vol. 43, No. 7, pp 708-714, July 1996.
6. D. Kajfez, "Dual resonance" IEEE Proceedings, vol. 135, Pt. H, No 2, pp 141-144, April 1988.
7. D. Kajfez, "Q-factor measurement with network analyzer", IEEE Transactions on microwave theory and techniques, vol. MTT-32, No. 7, pp 666-670, July 1984.
8. Ansys Software. Magneto-dynamic simulation. www.ansys.com